

Detailed experimental validation of a transient 3D thermal model with solar processor

Piet Standaert, Piet Houthuys, Jelle langmans, Wout Parys*
PHYSIBEL - building physics software, Ghent, Belgium
Ghent, Belgium, wout.parys@physibel.be

Abstract

The aim of the present paper is the validation of the transient 3D thermal model VOLTRA with experimental results. An insulated test box with one transparent side was constructed to generate two validation sets under: a) controlled conditions in a laboratory environment and b) outdoor conditions by field measurements. In the first indoors experiment the transient heat transfer due to a sudden internal power source was investigated. In the second experiment the box was put outdoors, allowing validating the solar processor module in VOLTRA. A good correspondence between the measured and simulated temperature distribution was found. The biggest deviations (still less than 10%) could be explained by the use of an empirical convection model for the air within the test box which doesn't take buoyancy-driven air flows into account.

1. Introduction

Advanced façade engineering often requires detailed transient thermal modelling in the design stage to predict energy performance, hygrothermal performance, thermal stresses and/or reaction to fire. Several numerical models exist today to simulate the thermal behavior of building components under dynamic excitation [1-6]. All these simulation tools have been developed trying to predict the real building component performance with the highest possible degree of detail. Nevertheless, every simulation model is by definition a simplification of reality in order to make them applicable in terms of simulation time and number of input parameters. For this reason, it is essential to understand the impact of the applied simplifications within the numerical model. The preferred way to investigate this impact is validation with experimental data. Several data-sets for the validation of 3D transient thermal models are available in the literature. Within the framework of multiple international research projects and networks, such as PASSYS, PASLINK and DYNASTEE, a wide range of experimental test-setups have been developed for the generation of validation data sets [7,8,9]. However, such data sets are not always public and/or documented in a way they can be easily used by external researchers.

The aim of the present article is two-fold: a) generate experimental data for the validation of advanced thermal modelling tools for the building sector and b) validation of the software tool VOLTRA against the measured data. The experimental validations were done in the framework of the SBO project IWT 050154 research program "Heat, air and moisture performance engineering. A whole building approach."

2. Numerical model: VOLTRA software package

The numerical model under investigation is the VOLTRA package from PHYSIBEL [6]. VOLTRA is a commercial thermal analysis program for transient heat transfer in three-dimensional rectangular objects. This building physics software tool is an extended version for time-dependent boundary conditions of the TRISCO package (for steady-state heat transfer) [10].

For the present study the VOLTRA software was extended with the RADCON module allowing to include non-linear radiation based on geometric view factors. In addition, the model is provided with an advanced solar simulator. The direct and diffuse solar radiation from climate data (e.g. as given in the European Test Reference Years) is cast on the material surfaces.

The direct solar irradiation is derived from the direct solar radiation on a horizontal surface and the position of the sun and taking sun obstacles into account. For the diffuse solar irradiation, the anisotropic diffuse model developed by Muneer [11], which also distinguishes between shaded and sunlit surfaces and between overcast and non-overcast conditions of the sunlit surfaces is implemented. The required input parameters are derived from sun position, slope, orientation, day of year, sunlit status, sky visibility, global and diffuse solar radiation data on a horizontal surface. Finally, also the radiation reflected from the ground in front of the surface is taking into account. This radiation is assumed to be isotropic and a function of the global solar radiation on a horizontal surface, the tilt of the surface, and the ground reflection factor, which can be defined as input for the model.

The absorbed solar radiation is converted to time dependent node powers, as additional boundary conditions to the system (external surfaces). Transmission of solar radiation is possible via transparent materials to simulate heat gains through transparent elements. The reflected solar radiation is diffuse and distributed according to the view factors (calculated with the RADCON module) to other material surfaces. This radiosity method, however, impedes the use of specular materials in internal zones (only diffuse reflection). Direct radiation is reflected (as diffuse radiation) using a reflection factor which may be function of the angle of incidence.

Application fields and reference research articles of VOLTRA simulation package:

- Advanced façade engineering;
- Transient analysis of thermal bridges [12,13];
- Dynamic thermal analysis of floor heating;
- Analysis of building elements exposed to fire (Eurocodes) [14,15];
- Thermal stress analysis [16];
- Ground heat losses (EN ISO 13370);
- Heat exchange problems (mass flows) [17];
- Passive solar building design (sunrooms, Trombe walls).

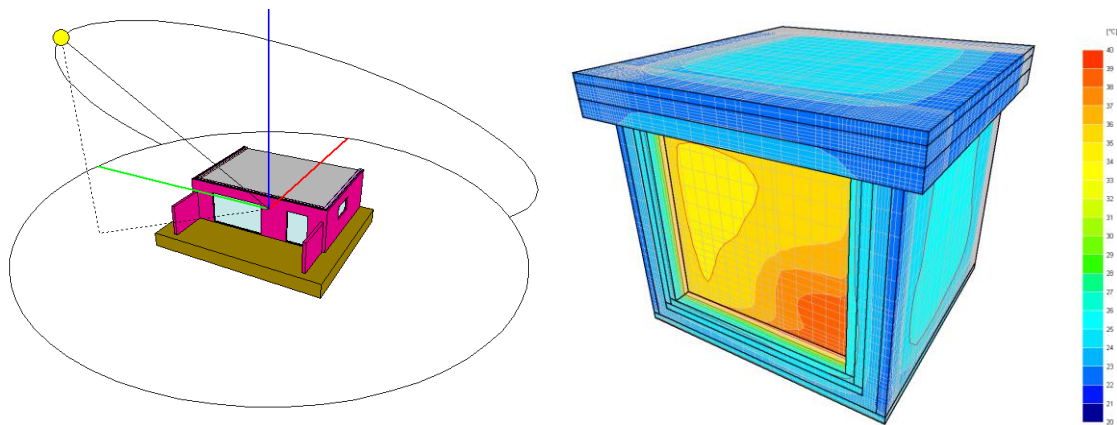


Figure 1: left) solar simulator within the VOLTRA package and right) example output: temperature distribution on external surface

3. Experimental study

For this validation exercise a test box has been constructed. This test box has been applied to generate two validation sets: 1) Controlled excitation under laboratory conditions and 2) free floating conditions under outdoor weather excitation. Both validation sets will be applied for comparison with the numerical model in paragraph 4.

3.1 Description of test box

A schematic overview of the test box with its dimensions and materials is given in Figure 2. The test box has a nearly cubic form, with interior dimensions of 46.8x47.6x41.6 cm³. The floor, roof and wall components of the box are all insulated with a 30mm extruded polystyrene. One side of the test box however contains a glazed surface with overall dimensions of 38.8x41.6cm². As part of this validation exercise the polystyrene insulation layer is not fully continuous inducing slight thermal bridging effects at the roof to wall joints and at the joints around the glazed surface (see Figure 2). The transparent side of the box has a double-glazing element (4-10-4) consisting of two clear glazing panels ($\tau=0.86$, $\alpha=0.06$, $\rho=0.08$). The gap (10 mm) between both glass layers (4 mm) is filled with air.

The materials were fixed using glue and thin nails with a negligible thermal effect. The purpose of the copper plate between the data logger space and the box above (Figure 4) is to create isothermal conditions below the floor insulation of the box. The measured temperature of this plate is used as a boundary condition in the simulations.

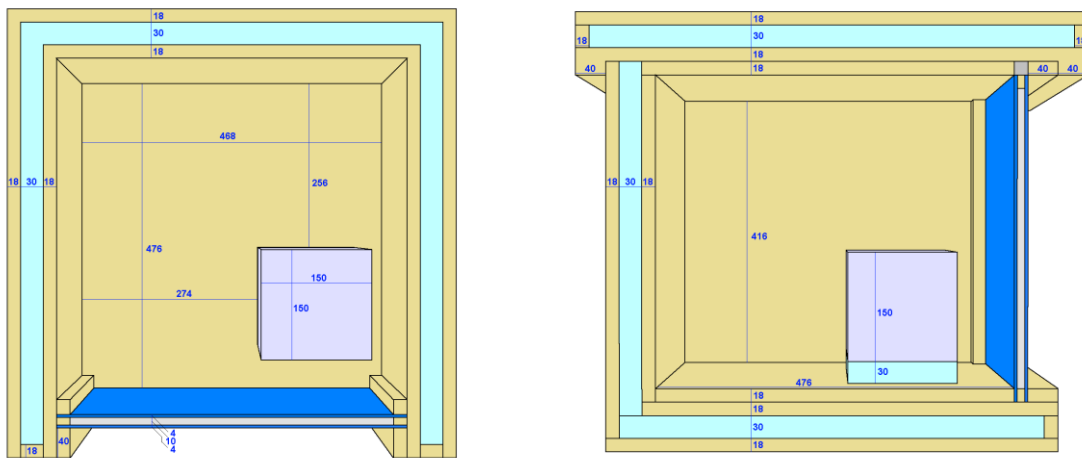


Figure 2: Materials and dimensions of test box: left) lower half box upper view and right) half box side view

The thermal properties are listed in Table 1. The thermal properties of the MDF and XPS layers have been measured with great detail at the laboratory of Building Physics of the KU Leuven as part of SBO project IWT 050154 research program "Heat, air and moisture performance engineering. A whole building approach.". The thermal properties of the other materials listed in Table 1 are adopted from [18].

	Thickness (mm)	Thermal conductivity (W/m/K)	Density (kg/m ³)	Heat capacity (J/kg/K)
Medium-density fibreboard (MDF)	18	0.0001.0+0.0928*	648	1450*
Extruded polystyrene (XPS)	30	0.0001.0+0.0309*	34.9	1470*
Soda lime	4	1.0	2500	650
Copper	1	380	8900	380

*properties measured at the Laboratory of Building Physics of KU Leuven

Table 1: Thermal properties of applied materials

The surface properties of the applied materials were also adopted from the literature. The long wave emissivity for soda lime was assumed $\epsilon = 0.95$ and $\epsilon = 0.90$ for all other materials. The solar absorptivity of the MDF surface was assumed $\alpha_s = 0.65$.

The test box was extensively equipped with fine thermocouples to registrate the thermal behaviour in great detail. Figure 3 below provides an overview of the location of the measuring points. The locations indicated with a coloured disk refer to a shielded thermocouple measuring the air temperature.

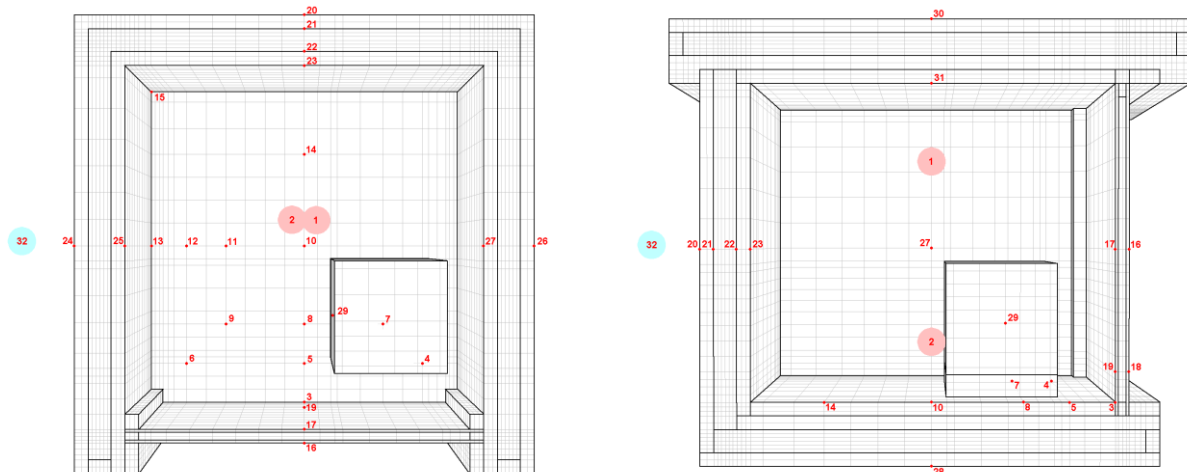


Figure 3: Locations of measuring points: left) lower half box upper view and right) half box side view.

3.2 Laboratory investigation

In a first step, laboratory measurements have been conducted under controlled conditions in the laboratory of Building Physics of the KU Leuven. Figure 4 shows the box which was equipped with a small copper box heater for this indoor experiment.

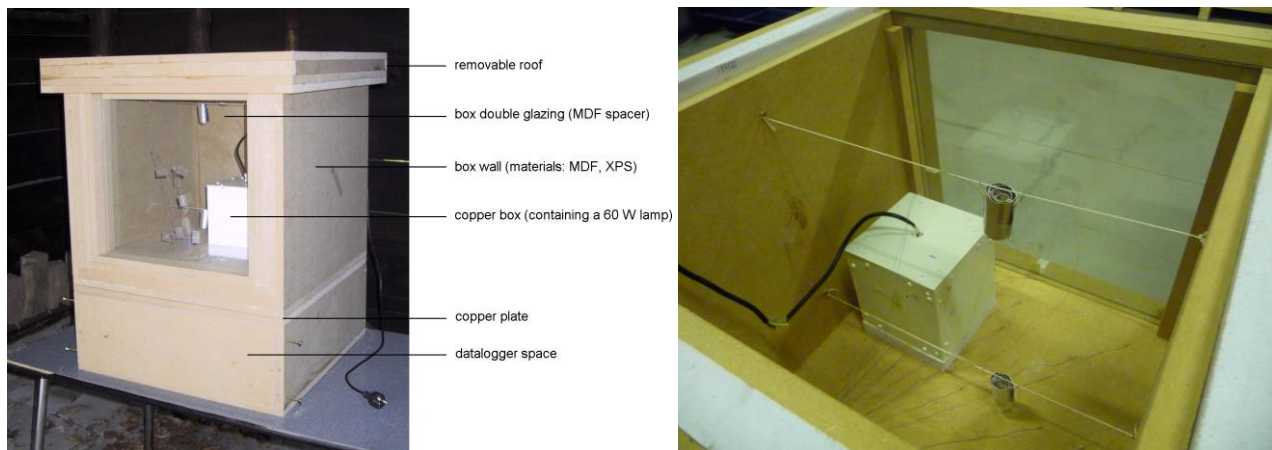


Figure 4: Picture of the test box equipped with the heater used in the indoor experiment: left) overall view and right) opened box.

The laboratory hall has a controlled indoor temperature (22°C-23°C). At the start of the experiment the heater inside the test box switched on, creating a constant power¹ of 57.8W. The thermal excitation of the test box was registered until equilibrium was established (2 days).

3.3 Field tests

For excitation under outdoor conditions the test box was installed in the test field of Laboratory of Building Physics of the KULeuven at Heverlee (Belgium). The box was put at 50°51'35" latitude and 4°40'44" longitude (Figure 5). The box was oriented to the South East (39.5 ° from South). Some buildings and trees in the environment obstruct the diffuse solar radiation.

¹ This power was measured using a "power consumption monitor" (La Crosse). A measurement with a GMC LonWorks U3681-V002

For the field tests the heater is omitted and the thermal excitation of the box was recorded under free floating conditions from 24 to 28 September.



Figure 5: Top left) Air view of the test site and Top right) View of the box on the test site and bottom) Panorama view from the box to its environment.

Boundary conditions

The climatic conditions near the test box were registered by the weather station of the VLIET-building [19] of the KU Leuven. However, this climate station in Heverlee didn't record the horizontal diffuse solar radiation, neither the infrared sky radiation. Therefore, these data were taken from the climate station in Limelette (about 20 km south of Heverlee). This method is justified by the close agreement between the air temperature courses and the horizontal global solar radiation courses at both sites.

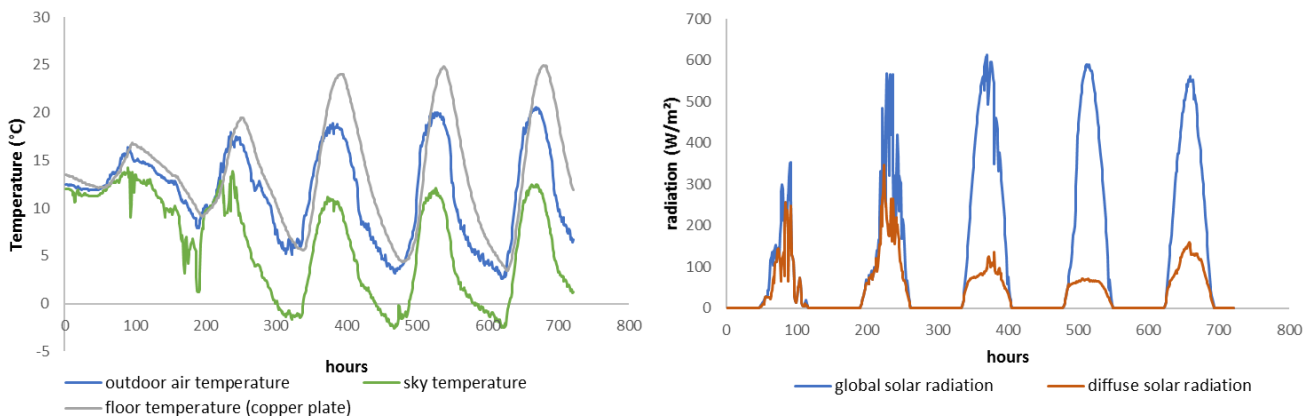


Figure 6: Ambient condition near the test box.

4. Validation of numerical model with experimental results

4.1 Laboratory experiment

Boundary conditions in numerical model

The 3 boundary conditions that fully determine the heat transfer in the box are (Figure):

- The laboratory temperature (thermocouple position 32). The air temperature and the mean wall surface temperatures are assumed to be the same. The radiation between the box surface elements and the

laboratory is calculated by VOLTRA (non-linear view factor-based radiation). The convection between the box surface elements is calculated empirically: $q_c = h_c(\theta_{air} - \theta_{surface})$ with $h_c = 1.46(\theta_{air} - \theta_{surface})^{1/3}$

A uniform convective heat transfer coefficient h_c is taken into account at each moment. Its value is based on the maximum difference between the air temperature and the box surface temperatures occurring.

- The copper plate temperature (thermocouple position 29). In the simulation, this temperature is imposed to the total surface. An additional steady state simulation was conducted in which the copper plate was included in the simulation assuming a constant temperature (23 °C) and a constant heat transfer coefficient (7.7 W/m²K) in the data logger zone. The temperature gradient on the copper plate is 1 °C only, which justifies the isothermal assumption.
- The power of the bulb used: 0 W for $t = 0$, and 56 W for $t > 0$.

Comparison of measured and simulated results

Figure 7 gives an illustration of the comparison between the measured and simulated temperatures for three sensor positions.

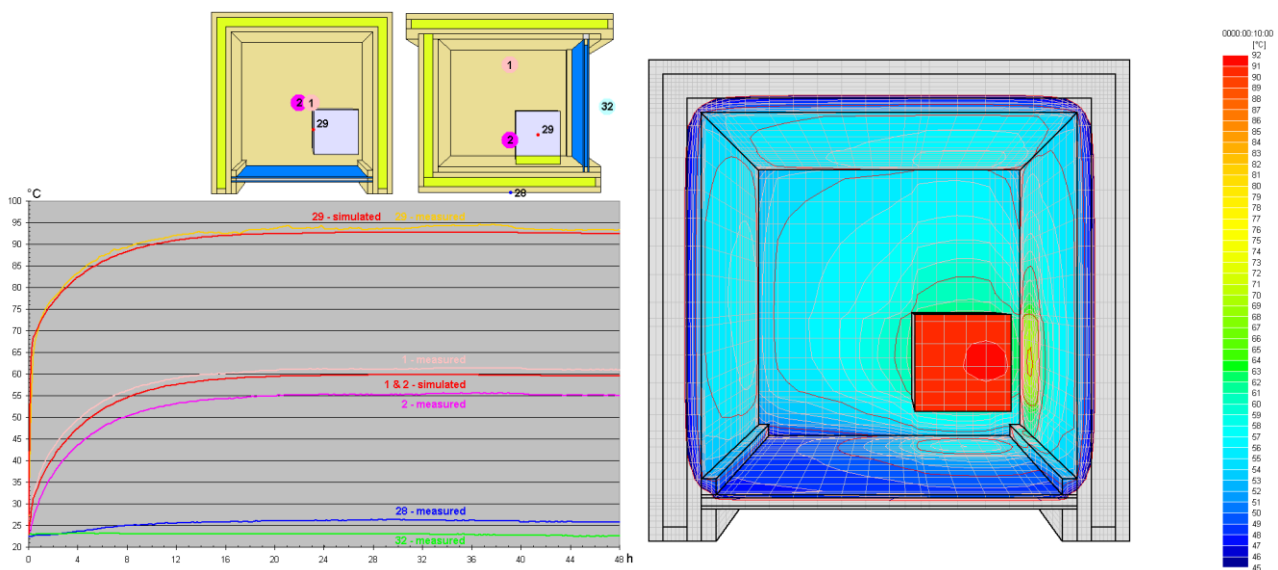


Figure 7: left) Measured and simulated temperatures (positions 1, 2, 28, 29 and 32) and right) Temperature distribution within the test box after equilibrium is reached.

The air temperatures measured at 2 levels (4 cm and 34 cm above the floor plate) show a considerable air temperature gradient (5.9 °C over 30 cm in steady state) due to the buoyancy. The simulation model however applies a single thermal air node assuming perfect mixing, as is common in building energy simulation. The simulated air temperature value lies in between these two measured temperature and smoothly follows the transient behaviour of the experiment (0-12h). Due to the air temperature gradient, the simulated temperatures at the floor level (3 up to 15) overestimate the measured ones, and the simulated temperature at the roof level (30) underestimates the measured one. The overestimation at the floor level is more important than the underestimation at the roof level. At the central level (positions 16, 17, 20, 21, 22, 23, 24, 25, 26, 27) the correspondence between simulated and measured temperatures is very good (≤ 0.5 °C). It can be expected that the air temperature gradient in the outdoors test will be much weaker. Indeed, the solar radiation will strike mainly the floor, and due to the heating up of the box by this 'floor heating' a weak temperature gradient can be expected.

4.2 Field tests

Boundary conditions in numerical model

The boundary conditions considered in the simulation of the field tests are the following:

- The outdoor air temperature (Heverlee) and the outdoor sky temperature (Limelette) (Figure 6). The radiation between the box roof surface and the outdoors is simulated (non-linear view factor-based

radiation) using the sky temperature. For the box walls the average of the sky temperature and the air temperature is used, taking into account that the walls look for 50 % to the sky and for 50% to the ground assumed at air temperature. The convection between the box surface elements is calculated empirically: $q_c = h_c(\theta_{air} - \theta_{surface})$ with $h_c = 8 \text{ W/m}^2\text{K}$. This value is representative for a wind speed of 1 m/s, which can be considered as the mean wind speed for the measured period;

- The copper plate temperature floor (thermocouple position 29): Figure 6;
- The horizontal global (Heverlee) and diffuse (Limelette) solar radiation: Figure 6.

Comparison of measured and simulated results

Figure 8 below illustrates the simulated isotherms on the external and internal surface of the test box for day 5. These plots illustrate the model's capability to handle solar heat gains in great detail.

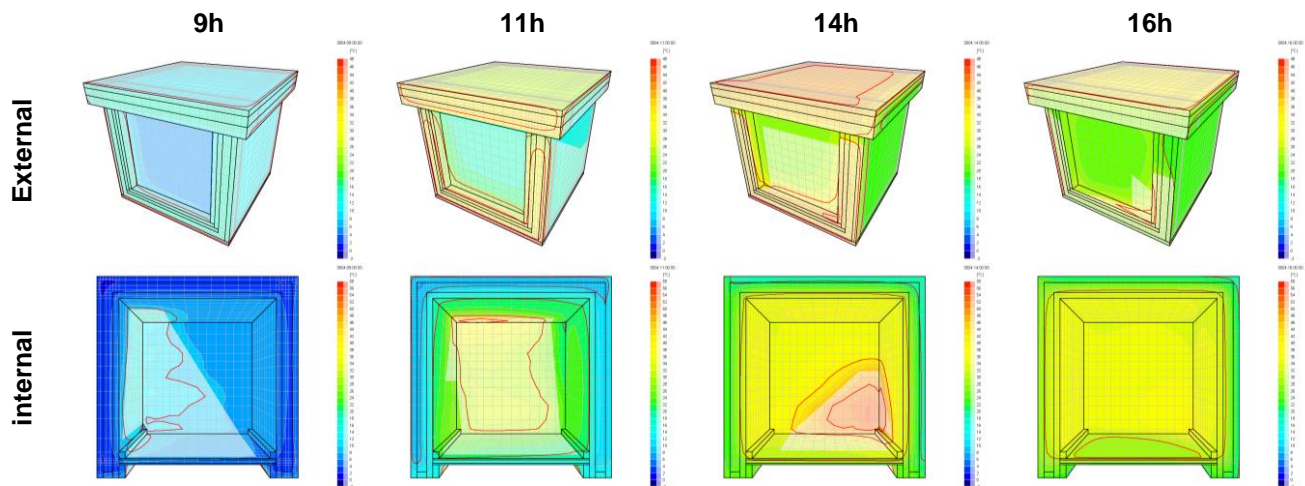


Figure 8: Simulated isotherms on day 5

The comparison of the measured and simulated temperatures is given in Figure 9 for 5 sensor positions:

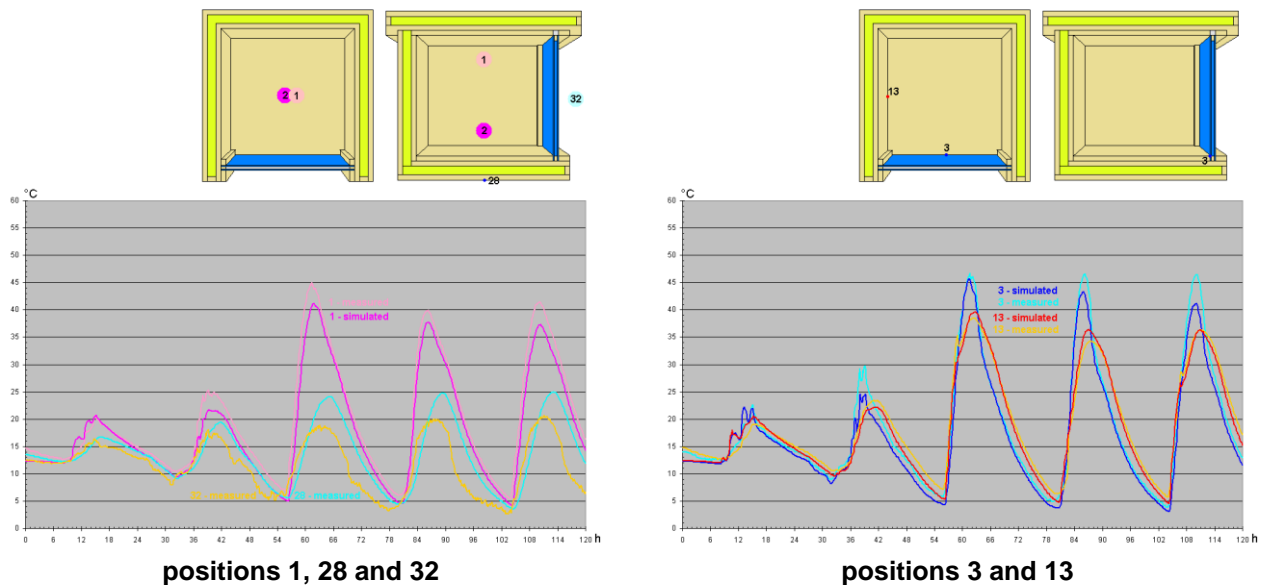


Figure 9: Measured and simulated temperatures.

The hypothesis for a less dominant air temperature gradient compared to the one in the internal power experiment couldn't be confirmed directly because of a sensor failure at location position 2. The fact that the

measured temperatures on the central floor (P10), on the central ceiling (P31) and in the higher air position (P2) are very close to each other (a difference of about 1 °C only occurs, except during a short noon period) confirms indirectly a weak air temperature gradient. The fact that the differences between measured and simulated temperatures all similar for all positions (and not higher for the floor positions as in the internal power experiment) is another indication of a weak air temperature gradient.

Generally spoken the overall correspondence between the measured and simulated temperature courses is good. The highest absolute differences occur in the early afternoon during the 3 last sunny days, which is normal because at that moment the highest temperature gradient (about 40 °C) occurs over the box.

The simulated air temperature is maximally 4.8 °C lower than the measured one. A possible explanation is the uniform convective heat transfer coefficient assumed in the simulation. At each moment a uniform coefficient $h_c = 1.72 \Delta\theta^{1/4}$ is used with $\Delta\theta$ being the maximum temperature difference between any surface element and the air occurring at that moment. The value is too high for most surfaces, which favours the cooling of the air.

The difference between the measured and the simulated temperatures is relatively large for the external surface points (16, 20, 24, 26 and 30). This can be explained by:

- The constant convective heat transfer coefficient (8 W/m²K) assumed. In reality the heat transfer coefficient depends on the variable wind speed, on the orientation and on natural convection. The coefficient seems underestimated for the southwest position and overestimated for the northeast position.
- The assumptions made for the infrared sky radiation for the vertical walls.
- A negligent fixing of a released thermocouple using a white tape caused the high difference (10 °C) for the external roof temperature (P30). Also at night the measured temperature on the roof is lower than the simulated one. Indeed, during the night there is no wind and a low convective heat transfer coefficient (for downwards heat transfer) is most probable.

The relatively large differences for the external surfaces are damped out inwards through the thermal insulation. This damping effect is lower for the double glazing and indeed also on the internal glazing surface an underestimation of 5 °C occurs.

A good correspondence between measurement and simulation is found for the floor positions. Temporary temperature fluctuations due to the absorbed solar radiation occur in both measured and simulated temperature courses (for example positions 10, 11, 12 and 15). Also, in the edge positions (3, 13 and 15) the correspondence is good.

The temperature courses in the positions 4, 5 and 6, compared to the ones in the positions 7, 8 and 9, show clearly that the effects of solar absorption, infrared radiation and 2D/3D conduction are simulated correctly.

5. Discussion and conclusions

It can be concluded that the correspondence between the measured and simulated temperature courses is good. The differences can be explained by the simplified empirical convection model, and by the inaccuracy of some of the boundary conditions. In conclusion it can be stated that the simulation of the transient 3D heat conduction, the infrared and solar radiation, and the convection using the VOLTRA package allows a high degree of precision. For investigations where an extremely high degree of accuracy would be required, additional research can be conducted to 1) provide a more precise predication of the boundary conditions and/or 2) a coupling with a CFD-model for the air zone.

6. References

- [1] Trechsel HR (2001) In: Trechsel HR, editor. Moisture analysis and condensation control in building envelopes: (MNL 40). ASTM International; 2001
- [2] Li Q, Rao J, Fazio P. Development of HAM tool for building envelope analysis. Build Environ May 2009;44:1065, p73.
- [3] Saber HH, Swinton MC, Kalinger P, Paroli RM. Long-term hygrothermal performance of white and black roofs in North American climates. Build Environ Apr. 2012; 50:141, p54.

- [4] Van Schijndel AWM. Modeling and solving building physics problems with FemLab. *Build Environ* Feb. 2003;38:319, p27.
- [5] Physibel (2017), manual BISTRA 4 computer program to calculate two-dimensional transient heat transfer in free-form objects
- [6] Physibel (2017), manual VOLTRA 8: computer program to calculate 3D & 2D transient heat transfer in objects described in a rectangular grid using the energy balance technique
- [7] Wouters P, Vandaele L, Voit P. Fisch N., The use of outdoor test cells for thermal and solar building research within the PASSYS project, Volume 28, Issue 2, April 1993, Pages 107-113
- [8] Baker P.H., van Dijk H.A.L., PASLINK and dynamic outdoor testing of building components, *Building and Environment*, Volume 43, Issue 2, February 2008, Pages 143-151
- [9] www.dynastee.info
- [10] Physibel (2017) manual TRISCO 13, computer program to calculate 3D & 2D steady state heat transfer in rectangular objects.
- [11] Muneer T. (1989) Algorithms for estimating hourly solar irradiation on slopes, *Building Serv. Eng. Res. Technol.* 10(2), p. 81-83
- [12] Mumovic, D., Ridley, I., Oreszczyn, T., & Davies, M. (2006). Condensation risk : comparison of steady-state and transient methods. *Building Serv.Eng.Res.Technol.*, 3, 219–233.
- [13] Martinez, R. G., Arrien, A. U., & Egaña, I. A. (2015). Calibration procedures for multidimensional heat transfer models based on on-site experimental data. *Energy Procedia*, 78, 3222–3227.
- [14] Ghazi Wakili, K., Wullschleger, L., & Hugi, E. (2008). Thermal behaviour of a steel door frame subjected to the standard fire of ISO 834: Measurements, numerical simulation and parameter study. *Fire Safety Journal*, 43(5), 325–333.
- [15] Ghazi Wakili, K., Hugi, E., Wullschleger, L., & Frank, T. (2007). Gypsum board in fire - Modeling and experimental validation. *Journal of Fire Sciences*, 25(3), 267–282.
- [16] Christen, R., Bergamini, A., & Ghazi Wakili, K. (2005). Low-temperature mechanical testing of full-scale prestressing systems. *Society for Experimental Mechanics*, 45(1), 35.
- [17] Jeong, Y. S., & Jung, H. K. (2015). Thermal Performance Analysis of Reinforced Concrete Floor Structure with Radiant Floor Heating System in Apartment Housing. *Advances in Materials Science and Engineering*, 2015.
- [18] Kumaran M. K. (1996), IEA Annex 24, Heat, air and moisture transfer in insulated envelope parts, Volume 3, Task 3: Material Properties. Reviewed by Per Jostein Hovde; edited by Fatin Ali Mohamed. Final
- [19] Desta, T. Z., Langmans, J., & Roels, S. (2011). Experimental data set for validation of heat, air and moisture transport models of building envelopes. *Building and Environment*, 46(5), 1038–1046.